GEOPHYSICAL RESEARCH LETTERS, VOL. 36, L13810, doi:10.1029/2009GL037435, 2009

Spectral absorption properties of aerosol particles from 350–2500nm

J. Vanderlei Martins,[1] Paulo Artaxo,[2] Yoram J. Kaufman,[3] Andrea D. Castanho,[2,4] and Lorraine A. Remer[3]

Received 30 January 2009; revised 22 April 2009; accepted 5 May 2009; published 14 July 2009.

[1] The aerosol spectral absorption efficiency (α_a in m^2/g) is measured over an extended wavelength range (350–2500 nm) using an improved calibrated and validated reflectance technique and applied to urban aerosol samples from Sao Paulo, Brazil and from a site in Virginia, Eastern US, that experiences transported urban/industrial aerosol. The average α_a values ($\sim$3m^2/g at 550 nm) for Sao Paulo samples are 10 times larger than α_a values obtained for aerosols in Virginia. Sao Paulo aerosols also show evidence of enhanced UV absorption in selected samples, probably associated with organic aerosol components. This extra UV absorption can double the absorption efficiency observed from black carbon alone, therefore reducing by up to 50% the surface UV fluxes, with important implications for climate, UV photolysis rates, and remote sensing from space. **Citation:** Martins, J. V., P. Artaxo, Y. J. Kaufman, A. D. Castanho, and L. A. Remer (2009), Spectral absorption properties of aerosol particles from 350–2500nm, *Geophys. Res. Lett.*, *36*, L13810, doi:10.1029/2009GL037435.

1. Introduction

[2] In recent years aerosol absorption, mainly by black carbon (BC), has been highlighted in climate change studies for its strong effects. BC absorbs solar energy over most of the solar spectrum, therefore, contrary to other aerosols (e.g., sulfates from urban pollution or even desert dust), BC acts like a greenhouse gas, and contributes to global warming. *Hansen and Sato* [2001] estimate a global average total forcing of non-absorbing aerosols of about –1.3 W/m^2 and the forcing due to black carbon of +0.8 W/m^2. The absorption properties of aerosol particles are still one of the largest uncertainties in estimating aerosol forcing of the climate. Global measurements of BC are not available and are badly needed. In situ aerosol absorption measurements are often inaccurate, and usually cover a narrow spectral range missing significant absorption features. This work presents spectral measurements of aerosol absorption efficiency in a broad spectral range (350–2500 nm) highlighting some characteristics of BC and other aerosol absorbers. We also discuss implications of these results to atmospheric studies. BC is the main absorbing material present in atmospheric aerosols, but it is not the only one. Soil dust absorbs light in the UV and visible, some organic materials absorb in the UV, and there is recent evidence that some organic materials also absorb light across the solar spectrum [*Kirchstetter et al.*, 2004].

2. Aerosol and BC Mass Absorption Efficiencies

[3] The interaction between aerosols and solar radiation in the Earth's atmosphere is well represented by three main parameters: the aerosol optical thickness (τ), the phase function, and the single scattering albedo (ω_o = ratio between scattering and extinction properties). Other representations of the particle properties can be more appropriate for specific applications. For instance, the mass scattering or absorption efficiencies (m^2/g) are the most appropriate parameters relating the aerosol mass (or particle mass emissions) with the particle optical properties. This is an essential connection between optics and aerosol transport and chemical models. Although optical measurements do not measure mass directly, the relationship between aerosol absorption and the mass of the absorber (BC for instance) is represented by the mass absorption efficiency. The aerosol absorption optical thickness (τ_{abs}) itself can be decomposed into aerosol absorption efficiency (α_a in m^2/g) multiplied by the aerosol total mass column per unit area (σ in g/m^2):

$$\tau_{abs} = \sigma \cdot \alpha_a \tag{1}$$

[4] As shown in equation (2), the aerosol mass absorption efficiency can be defined as the ratio between the aerosol absorption coefficient (β_a [m^{-1}]) and the aerosol mass concentration (M [g/m^3]). A similar definition can be applied to the BC mass absorption efficiency (α_{aBC}) by taking the ratio between β_a and the BC mass concentration (M_{BC} [g/m^3]). Also, α_a and α_{aBC} are related to each other by the fraction of BC mass to the total aerosol mass concentrations (r_{BC}).

$$\alpha_a = \frac{\beta_a}{M}, \tag{2}$$

and

$$\alpha_{aBC} = \frac{\beta_a}{M_{BC}} = \frac{\alpha_a}{r_{BC}} \tag{3}$$

Martins et al. [1998] show large variability for both α_{aBC} and r_{BC} for the Amazonian biomass burning aerosols (3–20 m^2/g and 2–15% respectively). Since the mass of black carbon cannot be measured directly, α_a is a more straightforward parameter to be measured and can be obtained by collecting aerosol particles on filters and measuring the collected aerosol mass and the light absorption on the filter. This work reports α_a results for aerosols from two areas

[1] Physics Department and Joint Center for Earth Systems Technology, University of Maryland Baltimore County, Baltimore, Maryland, USA.
[2] Institute of Physics, University of Sao Paulo, Sao Paulo, Brazil.
[3] NASA Goddard Space Flight Center, Greenbelt, Maryland, USA.
[4] Now at Department of Earth, Atmospheric, and Planetary Sciences, Massachusetts Institute of Technology, Cambridge, Massachusetts, USA.

0094-8276/09/2009GL037435$05.00

and will discuss some important characteristics of these aerosols.

3. In Situ Measurements of Aerosol Absorption Properties Using Filter Reflectance: Measurement and Calibration Methodologies

[5] Nuclepore filters are used to collect atmospheric aerosol particles and measure their mass concentration and spectral optical absorption properties. These filters have the important characteristic of collecting particles on the surface of the filter rather than having them embed inside the filter substrate (an effect commonly observed in quartz, Teflon, or paper filters). Measurements of embedded particles would exhibit artificially enhanced absorption due to multiple scattering inside the substrate.

[6] The Nuclepore filters are weighed before and after sampling using a high accuracy microbalance. The weighing procedure occurs after the filters are kept at low relative humidity (<50%) for over a week, and are subjected to irradiation by Po sources for the elimination of electrostatic charges. The filters are then placed on the top of a highly reflective (albedo ~1.0) lambertian spectralon panel, and their spectral reflectance is measured by an ASD (Analytical Spectral Devices) reflectance probe and spectrometer with nominal resolution of 1 nm between 350 to 2500 nm. Absorbing particles in contrast with bright surface backgrounds cause a strong reduction in the reflectance of the system (particle + surface) providing great sensitivity for this technique.

[7] The reflectance set-up consists of a pointed light source and a fiber optics probe connected to a detection spectrometer. The light source illuminates the filter with an average zenith angle (θ_o) of approximately 45°, while the probe receives the reflected light with an average zenith angle 10°, in the same azimuth. Thus the average scattering angle is approximately 145°. The reflectances of blank Nuclepore filters on the top of the same spectralon panel were used as the surface references for the measurement and quantification of loaded filters.

[8] We use a set of 23 Nuclepore calibration filters produced at the University of São Paulo, Brazil, using Monarch 71 black carbon particles manufactured by the Cabot Corporation [*Clarke et al.*, 1987; *Hitzenberger et al.*, 1996] with a large range of mass loadings to calibrate the system. The volume size distribution of the Monarch 71 particles peaks at 0.5 μm diameter, which is slightly higher than the peak of either urban pollution or biomass burning particles at roughly 0.3 to 0.4 μm. Figure 1 shows a plot of the measured mass density of each calibration filter (in units of m^2/g) as a function of the natural logarithm of the filter reflectance, normalized by the reflectance of a blank filter. The dashed line represents pure Lambert-Beer's law (equations (4), (5), and (6)) for the two way transmittance through the aerosol layer on the surface of the filter, multiplied by the previously measured surface reflectance of the blank Nuclepore filter on the top of the spectralon panel (ρ_{surf}). Since the particles are collected right on the surface of the Nuclepore filters, effects of the multiple scattering between the aerosol layer and the surface are minimized, and were basically neglected in the development of this simplified model. As shown in Figure 1 and confirmed by

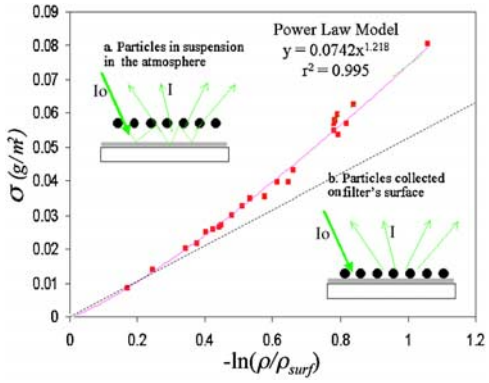

Figure 1. Measured relationship between the mass density of the standard BC samples versus the natural logarithm of the reflectance ratio (ρ/ρ_{surf}) at λ = 0.55 μm, for 23 filters with different mass loadings. Inserts on the left and right corner of the plot show a schematic comparison between (a) the atmospheric remote sensing case where particles are detached from the surface with important multiple reflections between the particles and the surface, versus (b) the filter case where particles are attached to the filter and this multiple reflection effect is suppressed.

radiative transfer calculations with DISORT [*Stamnes et al.*, 1988] (not shown) the Lambert-Beer's law is a good approximation for filters with low aerosol loading, represented here by values of $\ln(\rho/\rho_{surf})$ less than 0.25 in Figure 1.

$$\rho = \frac{I}{I_o} = \rho_{surf} \cdot \exp\left(-\frac{2\tau_{abs}}{G}\right) \tag{4}$$

Therefore,

$$-\ln\left(\rho/\rho_{Surf}\right) = \frac{2\tau_{abs}}{G} = \frac{2\sigma \cdot \alpha_a}{G} \tag{5}$$

which implies:

$$\sigma = -\frac{G}{2 \cdot \alpha_a} \ln\left(\rho/\rho_{Surf}\right) \tag{6}$$

where the total column mass density (σ) and the mass absorption efficiency (α_a) were defined previously, G is a geometric factor that depends on the effective illumination zenith angle (θo), and on the view zenith angle (θ). The application of this model will be tested and validated in the next section.

[9] For high loading cases, the shadowing between neighbor particles and other effects produce important deviations not accounted by Lambert-Beer's law. In order to compensate for these deviations an empirical scaling coefficient (b) is fitted to the data points, producing a power law correction on Lambert-Beer's law. Results of this power law are shown in Figure 1, fitting well on the top of the experimental data points. These corrections have been applied to all reflectance measurements with this particular reflectometer system.

[10] Equation (7) shows the addition of the empirical power law coefficient to the Lambert-Beer's Law function. Notice that the scaling coefficient b is the only change in the

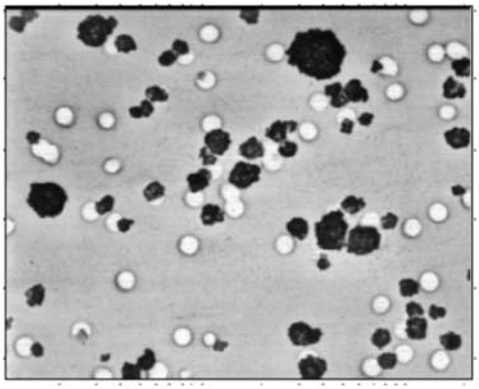

Figure 2. The picture shows a Scanning Electron Microscopy (SEM) photograph of a Nuclepore filter (pores in white, particles in black) containing the artificial BC particles used in the calibration of the reflectance technique. For scale purposes the pore diameters are in average 0.3 μm.

model as compared with equation (6). This result implies that the absorption efficiency (α_a) can still be determined as part of the slope of equation (7) similarly to the case for equation (6).

$$\sigma = -\frac{G}{2 \cdot \alpha_a}\left[\ln\left(\rho/\rho_{Surf}\right)\right]^b \qquad (7)$$

[11] Applying equation (7) to the power law fit result (Figure 1) assuming $G = 1$ for this particular geometry produces $\alpha_a = 6.7\ m^2/g$ for the Monarch 71 samples. This result is consistent with previously published results for Monarch 71 particles and our Mie calculations of the mass absorption efficiency of these particles:

[12] 1) Monarch 71 samples measured by *Clarke et al.* [1987] show $\alpha_a = 6.4 \pm 0.3$ m^2/g (considering results from Nuclepore filters with particles in the same size range as here), and *Hitzenberger et al.* [1996] present $\alpha_a = 6.6 \pm 1.0$ m^2/g, both in good agreement with the 6.7 m^2/g results obtained from the power law slope in Figure 1 and equation (7).

[13] 2) Using a 6.8 m^2/g calibration coefficient obtained from the same standard filters plotted in Figure 1, the paper by *Reid et al.* [1998] shows an absolute validation of the reflectance technique discussed here by comparing it with an standard extinction cell plus nephelometer for several samples of biomass burning aerosols collected in the Amazon region, in Brazil. The reflectance results were in excellent agreement with the extinction cell measurements for a large range of aerosol loading.

[14] 3) Our results are also in agreement with the theoretical modeling of the Monarch 71 particle properties using the measured size distribution by SEM (scanning electron microscopy) and pure BC refractive indices, which provided an estimated absorption efficiency of 6.8 m^2/g, discussed in more details below. A scanning electron microscope (SEM) picture of the Monarch 71 sample collected on a Nuclepore filter is shown in Figure 2. Although Mie calculations of absorption and scattering coefficients rely on many assumptions (refractive indices, size distribution, particle homogeneity and shape, etc.) and often do not provide realistic results, this particular case is in excellent agreement with the literature and with the results presented here.

4. Results From Urban Aerosol Samples

4.1. Spectral Absorption Efficiency of Sao Paulo Aerosols

[15] Sao Paulo is a major urban center with about 18 million people in the metropolitan area. The main sources of pollution are widespread trucks, buses, cars, and industries. Sao Paulo has a relatively old fleet of transportation vehicles and due to little (or no) control on vehicular emission and the low technology applied to engines and industrial processes, the locally generated aerosol can be quite absorbing. The AERONET Sunphotometer located in Sao Paulo shows single scattering albedo at 0.55 μm varying from 0.76 up to 0.96 during the winter time. Lower single scattering albedo represents higher concentration of BC and proportionally larger aerosol absorption efficiency.

[16] Aerosol samples were collected every 12 hours in the fine mode (diameter <2.5 μm) Nuclepore filters during the local winter time (July–August 1999). These filters were submitted to gravimetric analysis before and after sampling, and were analyzed by the spectral absorption reflectance technique described above. Eleven randomly selected filters collected during this period were analyzed and used to create the mean spectral absorption efficiency of the fine mode aerosols shown by the red curve in Figure 3. The yellow area indicates the standard deviation of the curves measured during that winter. Fine mode aerosols, basically follow a spectral dependence similar to $1/\lambda$ from 400 to 2100 nm, denoted by the blue curve in Figure 3.

[17] Figure 3 also shows the average and standard deviation (pink) values obtained at the Wallops Flight Facility on the Virginia Coast during the CLAMS (Chesapeake Lighthouse & Aircraft Measurements for Satellites) experiment

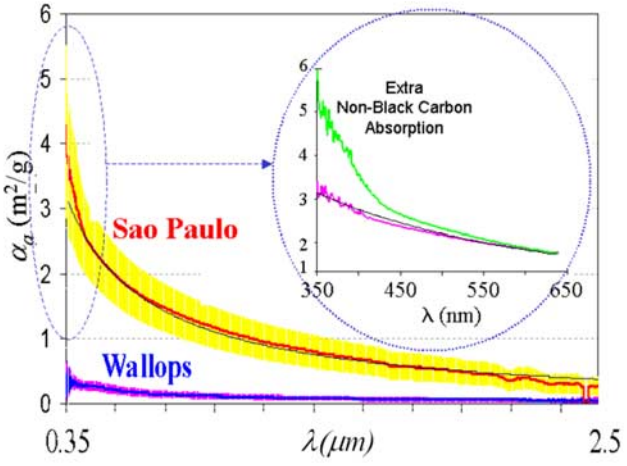

Figure 3. Average and standard deviation of the spectral absorption efficiencies for Sao Paulo (red and yellow) and for the east coast of the United States (blue and pink), for particles with diameter smaller that 2.5 μm. The blue line over the Sao Paulo curve corresponds to $1/\lambda$ spectral dependence. The figure excerpt shows α_a for two individual days in Sao Paulo with and without the enhanced UV absorption.

Table 1. Effect of the Excess UV Absorption as Seen by the Set of Sao Paulo Curves Seen in the Inset of Figure 3 in Reducing the Downward Solar UV Flux at the Surface[a]

λ(nm)	ωo	τ	g	TOA dwd Flux/Surf dwd Flux (W/m^2/μm)	% Extra Reduction
b. 550	0.80	0.40	0.60		
b. 440	0.81	0.59	0.65		
b. 350	0.83	0.84	0.70	590/230	
e. 350	0.73	0.96	0.70	590/179	22
b. 300	0.85	1.12	0.73	183/0.357	
e. 300	0.76	1.26	0.73	183/0.177	50

[a]The labels b. and e. indicate baseline and enhanced UV absorption, respectively.

during June and July 2001. The Wallops curve in Figure 3 represents statistics of a total of 45 filters for particles with diameters less than 2.5 μm, and changed every 12 hours. All filters collected were analyzed and contributed to the curve in Figure 3. The Wallops aerosols represent locally emitted rural and marine aerosols, and episodes of long distance transport of urban/industrial pollution from the Ohio valley and other industrial and population centers of the eastern portion of the U.S. During the CLAMS experiment approximately 1/3 of the sampling days experienced elevated fine particle mass concentrations of over 15 μg/m^3 or $\tau > 0.30$ [*Castanho et al.*, 2005].

[18] Figure 3 contains several important results. First, the Sao Paulo aerosols show absorption efficiency 10 times larger then the Wallops particles. Second, the $1/\lambda$ spectral dependence (solid blue curve) holds very well for the average Sao Paulo aerosol in a very wide spectral range, from 400–2100 nm, which is compatible with expected BC absorption present in relatively small particles. Finally, the average Sao Paulo aerosols show significant enhancement in the UV absorption efficiency indicating larger imaginary refractive index in that range. This UV feature is emphasized in the Figure 3 excerpt, which shows α_a for two individual days in Sao Paulo (pink and green lines), as well as a $1/\lambda$ curve (continuous blue line) expected for absorption by pure BC particles. The enhanced UV absorption feature occurred in 4 of the 11 Sao Paulo cases. The case with extra UV absorption in Figure 3 shows about twice as much absorption as the one expected for pure BC particles, corresponding to an increase in the imaginary refractive index for the UV range. *Jacobson* [1999] shows several "nitrated and/or aromatic particulate organic substances observed in the atmosphere or in emissions" that contain UV absorption exactly in the range of the observations in Sao Paulo. *Kirchstetter et al.* [2004] show strong spectral dependence on the light absorption by organic aerosols in the UV. The production of these compounds and their day-to-day variability still needs further understanding, but will not be explored in this work.

4.2. Effects of Enhanced UV Absorption by Organic Aerosols

[19] The Santa Barbara DISORT Radiative Transfer (SBDART) model [*Ricchiazzi et al.*, 1998] was used to calculate the effect of the enhanced absorption by organic aerosols on the UV radiative fluxes at the top and bottom of the atmosphere. First, aerosol optical properties in the UV spectral range were required. We used retrievals from the Aerosol Robotics NETwork (AERONET) instrument located in Sao Paulo. AERONET is a global network of sun/sky radiometers that provide retrievals of total column aerosol properties, including ω_o [*Dubovik and King*, 2000]. The shortest wavelength of ω_o and asymmetry parameter (g) that AERONET derives is at 440 nm. AERONET results from Sao Paulo show 440 nm ω_o values ranging from 0.76 to 0.96. Assuming AERONET imaginary and real refractive indices are constant from 440 nm throughout the UV, and using an average aerosol size distribution, values of τ, ω_o and g derived at 440 nm were extrapolated to 300 and 350 nm for the baseline case (no enhanced UV absorption), as indicated in Table 1. Then, starting from this baseline and assuming the absorption enhancement shown in Figure 3, new ω_o values were calculated for the high UV absorbing case. Due to multiple scattering effects, aerosol absorption is a very efficient suppressant of UV photons. Table 1 summarizes the studied cases and the effect of the enhanced absorption on the downward UV flux for the baseline and enhanced models (labeled b. and e., respectively), using the given ω_o, τ, asymmetry parameter (g), and surface albedo equal to 0.05. The excess UV absorption contributed to reducing ω_o and increasing the total aerosol optical thickness as indicated in Table 1. Higher surface albedo, lower ω_o, or higher τ, will produce stronger absorption effects. The total effect in the downward UV flux at the surface is indicated for the two wavelengths (350 and 300 nm) showing, respectively, an extra 22 and 50% decrease in UV flux due to the extra UV absorption. Top of the atmosphere (TOA) values of UV fluxes are also shown as a reference. This reduction has an impact on atmospheric photochemical and biological processes. The results presented for 300 nm may be conservative due to the assumption of constant absorption efficiency between 350 and 300 nm. Looking at Figure 3 the absorption efficiency tendency appears to increase towards shorter wavelengths, which could potentially increase even further the enhanced UV absorption. Additional measurements are needed in shorter wavelengths in order to complement and better understand these results.

5. Discussion and Conclusion

[20] The accurate spectral absorption measurements performed in this work are important for a full characterization of the aerosol radiative effects over the solar spectrum. The factor of 10 larger absorption efficiency observed in Sao Paulo versus Virginia, corresponds to a lower single scattering albedo, and higher BC emissions. These characteristics are usually associated with lower technology applied in engines and industries, as well as domestic activities.

[21] The UV results show an important example of UV absorbing aerosols, most likely organics, produced occasionally over the Sao Paulo metropolitan area that significantly

reduce surface UV fluxes. This enhanced absorption can reduce surface UV radiative fluxes by 50%. Such a large decrease in UV at the surface suggests potentially large effects on photochemistry and biological processes. More measurements are still needed in shorter UV wavelengths to fully characterize this issue.

[22] **Acknowledgments.** We thank the Electron Microscopy Laboratory of the Institute of Physics of the University of Sao Paulo (IFUSP) for the picture in Figure 2, Ana Lucia Loureiro for the preparation of the BC standard samples and Tarsis Germano for help with the reflectance analyses, both from IFUSP. We also would like to thank the work of Marcia Yamasoe, Artemio Fattori, and Ken Rutledge and his team, for contributing to the aerosol collection during the CLAMS experiment. J. V. Martins was funded by the NASA Atmospheric Composition and Radiation Science Programs, grants NNG04GH65G, NNX07AT47G, and NNX08AJ78G.

References

Castanho, A., J. V. Martins, P. V. Hobbs, P. Artaxo, L. A. Remer, and M. Yamasoe (2005), Chemical characterization of aerosols on the east coast of the United States using aircraft and ground based stations during the CLAMS experiment, *J. Atmos. Sci.*, *62*, 934–946.

Clarke, A. D., K. J. Noone, J. Heintzenberg, S. G. Warren, and D. S. Covert (1987), Aerosol light absorption measurement techniques: Analysis and intercomparisons, *Atmos. Environ.*, *21*, 1455–1465.

Dubovik, O., and M. D. King (2000), A flexible inversion algorithm for retrieval of aerosol optical properties from Sun and sky radiance measurements, *J. Geophys. Res.*, *105*, 20,673–20,696.

Hansen, J. E., and M. Sato (2001), Trends of measured climate forcing agents, *Proc. Natl. Acad. Sci. U. S. A.*, *98*, 14,778–14,783, doi:10.1073/pnas.261553698.

Hitzenberger, R., U. Dusek, and A. Berner (1996), Black carbon measurements using an integrating sphere, *J. Geophys. Res.*, *101*, 19,601–19,606.

Jacobson, M. Z. (1999), Isolating nitrated and aromatic aerosols and nitrated aromatic gases as sources of ultraviolet light absorption, *J. Geophys. Res.*, *104*, 3527–3542.

Kirchstetter, T. W., T. Novakov, and P. V. Hobbs (2004), Evidence that the spectral dependence of light absorption by aerosols is affected by organic carbon, *J. Geophys. Res.*, *109*, D21208, doi:10.1029/2004JD004999.

Martins, J. V., P. Artaxo, C. Liousse, J. S. Reid, P. V. Hobbs, and Y. J. Kaufman (1998), Effects of black carbon content, particle size, and mixing on light absorption by aerosols from biomass burning in Brazil, *J. Geophys. Res.*, *103*, 32,041–32,050.

Reid, J. S., P. V. Hobbs, C. Liousse, J. V. Martins, R. E. Weiss, and T. F. Eck (1998), Comparisons of techniques for measuring shortwave absorption and black carbon content of aerosols from biomass burning in Brazil, *J. Geophys. Res.*, *103*, 32,031–32,040.

Ricchiazzi, P., S. R. Yang, C. Gautier, and D. Sowle (1998), SBDART: A research and teaching software tool for plane-parallel radiative transfer in the Earth's atmosphere, *Bull. Am. Meteorol. Soc.*, *79*, 2101–2114.

Stamnes, K., S.-C. Tsay, W. Wiscombe, and K. Jayaweera (1988), A numerically stable algorithm for discrete-ordinate-method radiative transfer in multiple scattering and emitting layered media, *Appl. Opt.*, *27*, 2502–2509.

P. Artaxo, Institute of Physics, University of Sao Paulo, Caixa Postal 66318, Sao Paulo CEP 05315-970, Brazil.

A. D. Castanho, Department of Earth, Atmospheric, and Planetary Sciences, Massachusetts Institute of Technology, 77 Massachusetts Avenue, Cambridge, MA 02139, USA.

Y. J. Kaufman and L. A. Remer, NASA Goddard Space Flight Center, Code 613.2, Greenbelt, MD 20771, USA.

J. V. Martins, Physics Department, University of Maryland Baltimore County, 1000 Hilltop Circle, Baltimore, MD 21250, USA. (martins@umbc.edu)